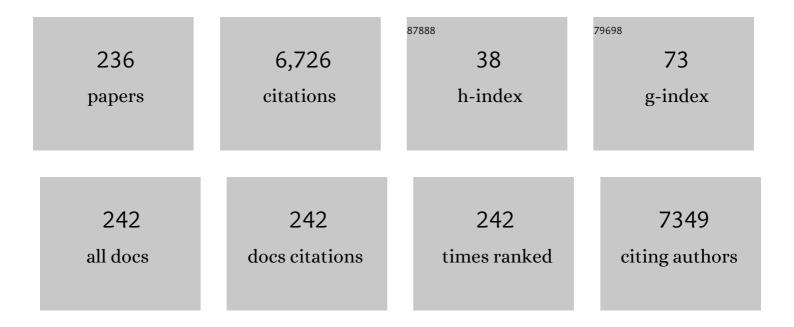
Frans N Van De Vosse

List of Publications by Year in descending order

Source: https://exaly.com/author-pdf/4351363/publications.pdf Version: 2024-02-01



#	Article	IF	CITATIONS
1	Experimental investigation of collagen waviness and orientation in the arterial adventitia using confocal laser scanning microscopy. Biomechanics and Modeling in Mechanobiology, 2012, 11, 461-473.	2.8	845
2	Pulse Wave Propagation in the Arterial Tree. Annual Review of Fluid Mechanics, 2011, 43, 467-499.	25.0	287
3	Coronary Thermodilution to Assess Flow Reserve. Circulation, 2002, 105, 2482-2486.	1.6	279
4	AN APPROXIMATE PROJECTION SCHEME FOR INCOMPRESSIBLE FLOW USING SPECTRAL ELEMENTS. International Journal for Numerical Methods in Fluids, 1996, 22, 673-688.	1.6	220
5	Epicardial Stenosis Severity Does Not Affect Minimal Microcirculatory Resistance. Circulation, 2004, 110, 2137-2142.	1.6	210
6	A patient-specific computational model of fluid–structure interaction in abdominal aortic aneurysms. Medical Engineering and Physics, 2005, 27, 871-883.	1.7	161
7	The mechanical role of thrombus on the growth rate of an abdominal aortic aneurysm. Journal of Vascular Surgery, 2010, 51, 19-26.	1.1	138
8	Direct Volumetric Blood Flow Measurement in Coronary Arteries by Thermodilution. Journal of the American College of Cardiology, 2007, 50, 2294-2304.	2.8	132
9	A fluid–structure interaction method with solid-rigid contact for heart valve dynamics. Journal of Computational Physics, 2006, 217, 806-823.	3.8	123
10	The influence of boundary conditions on wall shear stress distribution in patients specific coronary trees. Journal of Biomechanics, 2011, 44, 1089-1095.	2.1	116
11	A wave propagation model of blood flow in large vessels using an approximate velocity profile function. Journal of Fluid Mechanics, 2007, 580, 145-168.	3.4	111
12	Effects of Wall Calcifications in Patient-Specific Wall Stress Analyses of Abdominal Aortic Aneurysms. Journal of Biomechanical Engineering, 2007, 129, 105-109.	1.3	101
13	"Virtual―(Computed) FractionalÂFlowÂReserve. JACC: Cardiovascular Interventions, 2015, 8, 1009-1017.	2.9	100
14	Experimental validation of a time-domain-based wave propagation model of blood flow in viscoelastic vessels. Journal of Biomechanics, 2008, 41, 284-291.	2.1	93
15	Steady entry flow in a curved pipe. Journal of Fluid Mechanics, 1987, 177, 233-246.	3.4	90
16	Dependence of Intramyocardial Pressure and Coronary Flow on Ventricular Loading and Contractility: A Model Study. Annals of Biomedical Engineering, 2006, 34, 1833-1845.	2.5	85
17	A pulse wave propagation model to support decision-making in vascular access planning in the clinic. Medical Engineering and Physics, 2012, 34, 233-248.	1.7	77
18	Validation of a Fluid–Structure Interaction Model of a Heart Valve using the Dynamic Mesh Method in Fluent. Computer Methods in Biomechanics and Biomedical Engineering, 2004, 7, 139-146.	1.6	74

#	Article	IF	CITATIONS
19	A Mathematical Model to Evaluate Control Strategies for Mechanical Circulatory Support. Artificial Organs, 2009, 33, 593-603.	1.9	72
20	Patient-Specific AAA Wall Stress Analysis: 99-Percentile Versus Peak Stress. European Journal of Vascular and Endovascular Surgery, 2008, 36, 668-676.	1.5	70
21	Plaque and shear stress distribution in human coronary bifurcations: a multislice computed tomography study. EuroIntervention, 2009, 4, 654-661.	3.2	70
22	3D fusion of intravascular ultrasound and coronary computed tomography for in-vivo wall shear stress analysis: a feasibility study. International Journal of Cardiovascular Imaging, 2010, 26, 781-796.	1.5	69
23	Validation of a patient-specific hemodynamic computational model for surgical planning of vascular access in hemodialysis patients. Kidney International, 2013, 84, 1237-1245.	5.2	67
24	The Influence of Wall Stress on AAA Growth and Biomarkers. European Journal of Vascular and Endovascular Surgery, 2010, 39, 410-416.	1.5	63
25	Theoretical models for coronary vascular biomechanics: Progress & challenges. Progress in Biophysics and Molecular Biology, 2011, 104, 49-76.	2.9	62
26	MRI-based quantification of outflow boundary conditions for computational fluid dynamics of stenosed human carotid arteries. Journal of Biomechanics, 2010, 43, 2332-2338.	2.1	61
27	Toward Noninvasive Blood Pressure Assessment in Arteries by Using Ultrasound. Ultrasound in Medicine and Biology, 2011, 37, 788-797.	1.5	61
28	Biomechanical properties of abdominal aortic aneurysms assessed by simultaneously measured pressure and volume changes in humans. Journal of Vascular Surgery, 2008, 48, 1401-1407.	1.1	55
29	A physiologically representativein vitromodel of the coronary circulation. Physiological Measurement, 2004, 25, 891-904.	2.1	53
30	A method for the quantification of the pressure dependent 3D collagen configuration in the arterial adventitia. Journal of Structural Biology, 2012, 180, 335-342.	2.8	53
31	Towards model-based analysis of cardiac MR tagging data: Relation between left ventricular shear strain and myofiber orientation. Medical Image Analysis, 2006, 10, 632-641.	11.6	52
32	Non-linear viscoelastic behavior of abdominal aortic aneurysm thrombus. Biomechanics and Modeling in Mechanobiology, 2008, 7, 127-137.	2.8	51
33	A lumped parameter model of cerebral blood flow control combining cerebral autoregulation and neurovascular coupling. American Journal of Physiology - Heart and Circulatory Physiology, 2012, 303, H1143-H1153.	3.2	51
34	Myocardial resistance assessed by guidewire-based pressure-temperature measurement: In vitro validation. Catheterization and Cardiovascular Interventions, 2004, 62, 56-63.	1.7	48
35	Effects of exercise modalities on central hemodynamics, arterial stiffness and cardiac function in cardiovascular disease: Systematic review and meta-analysis of randomized controlled trials. PLoS ONE, 2018, 13, e0200829.	2.5	46
36	Buffers Strongly Modulate Fibrin Self-Assembly into Fibrous Networks. Langmuir, 2017, 33, 6342-6352.	3.5	45

#	Article	IF	CITATIONS
37	Patient Specific Wall Stress Analysis and Mechanical Characterization of Abdominal Aortic Aneurysms Using 4D Ultrasound. European Journal of Vascular and Endovascular Surgery, 2016, 52, 635-642.	1.5	44
38	Continuous infusion thermodilution for assessment of coronary flow: Theoretical background and in vitro validation. Medical Engineering and Physics, 2009, 31, 688-694.	1.7	42
39	Cardiovascular models for personalised medicine: Where now and where next?. Medical Engineering and Physics, 2019, 72, 38-48.	1.7	42
40	A numerical and experimental analysis of the flow field in a two-dimensional model of the human carotid artery bifurcation. Journal of Biomechanics, 1987, 20, 499-509.	2.1	40
41	Mixing of non-Newtonian fluids in time-periodic cavity flows. Journal of Non-Newtonian Fluid Mechanics, 2000, 93, 265-286.	2.4	40
42	Pump Flow Estimation From Pressure Head and Power Uptake for the HeartAssist5, HeartMate II, and HeartWare VADs. ASAIO Journal, 2013, 59, 420-426.	1.6	40
43	A finite element analysis of the steady laminar entrance flow in a 90° curved tube. International Journal for Numerical Methods in Fluids, 1989, 9, 275-287.	1.6	39
44	Estimation of distributed arterial mechanical properties using a wave propagation model in a reverse way. Medical Engineering and Physics, 2010, 32, 957-967.	1.7	39
45	Continuous-Flow Cardiac Assistance: Effects on Aortic Valve Function in a Mock Loop. Journal of Surgical Research, 2011, 171, 443-447.	1.6	39
46	A constitutive model for developing blood clots with various compositions and their nonlinear viscoelastic behavior. Biomechanics and Modeling in Mechanobiology, 2016, 15, 279-291.	2.8	39
47	What is needed to make cardiovascular models suitable for clinical decision support? A viewpoint paper. Journal of Computational Science, 2018, 24, 68-84.	2.9	39
48	A three-dimensional fluid–structure interaction method for heart valve modelling. Comptes Rendus - Mecanique, 2005, 333, 856-866.	2.1	37
49	A Novel Angiographic Quantification ofÂAortic Regurgitation After TAVR Provides an Accurate Estimation of Regurgitation Fraction Derived From Cardiac Magnetic Resonance Imaging. JACC: Cardiovascular Interventions, 2018, 11, 287-297.	2.9	37
50	A novel passive left heart platform for device testing and research. Medical Engineering and Physics, 2015, 37, 361-366.	1.7	36
51	Chaotic fluid mixing in non-quasi-static time-periodic cavity flows. International Journal of Heat and Fluid Flow, 2000, 21, 176-185.	2.4	35
52	Quantification of aortic stiffness and wall stress in healthy volunteers and abdominal aortic aneurysm patients using time-resolved 3D ultrasound: a comparison study. European Heart Journal Cardiovascular Imaging, 2019, 20, 185-191.	1.2	35
53	A model for arterial adaptation combining microstructural collagen remodeling and 3D tissue growth. Biomechanics and Modeling in Mechanobiology, 2010, 9, 671-687.	2.8	34
54	Periprocedural variations of platelet reactivity during elective percutaneous coronary intervention. Journal of Thrombosis and Haemostasis, 2012, 10, 2452-2461.	3.8	34

#	Article	IF	CITATIONS
55	Droplet behavior in the presence of insoluble surfactants. Physics of Fluids, 2004, 16, 2785-2796.	4.0	33
56	A Numerical Method of Reduced Complexity for Simulating Vascular Hemodynamics Using Coupled 0D Lumped and 1D Wave Propagation Models. Computational and Mathematical Methods in Medicine, 2012, 2012, 1-10.	1.3	33
57	A mock circulation model for cardiovascular device evaluation. Physiological Measurement, 2014, 35, 687-702.	2.1	31
58	Intra-aortic balloon counterpulsation reduces mortality in large anterior myocardial infarction complicated by persistent ischaemia: a CRISP-AMI substudy. EuroIntervention, 2015, 11, 286-292.	3.2	30
59	Applicability of the polynomial chaos expansion method for personalization of a cardiovascular pulse wave propagation model. International Journal for Numerical Methods in Biomedical Engineering, 2014, 30, 1679-1704.	2.1	29
60	Small coronary calcifications are not detectable by 64-slice contrast enhanced computed tomography. International Journal of Cardiovascular Imaging, 2011, 27, 143-152.	1.5	27
61	A generic constitutive model for the passive porcine coronary artery. Biomechanics and Modeling in Mechanobiology, 2011, 10, 249-258.	2.8	27
62	Patient-Specific Computational Modeling of Upper Extremity Arteriovenous Fistula Creation: Its Feasibility to Support Clinical Decision-Making. PLoS ONE, 2012, 7, e34491.	2.5	27
63	A sensitivity analysis of a personalized pulse wave propagation model for arteriovenous fistula surgery. Part A: Identification of most influential model parameters. Medical Engineering and Physics, 2013, 35, 810-826.	1.7	27
64	Application of an Adaptive Polynomial Chaos Expansion on Computationally Expensive Three-Dimensional Cardiovascular Models for Uncertainty Quantification and Sensitivity Analysis. Journal of Biomechanical Engineering, 2016, 138, .	1.3	26
65	Toward the detection of intraplaque hemorrhage in carotid artery lesions using photoacoustic imaging. Journal of Biomedical Optics, 2016, 22, 041010.	2.6	26
66	A finite element approximation of the unsteady two-dimensional Navier-Stokes equations. International Journal for Numerical Methods in Fluids, 1986, 6, 427-443.	1.6	25
67	Influence of dilated cardiomyopathy and a left ventricular assist device on vortex dynamics in the left ventricle. Computer Methods in Biomechanics and Biomedical Engineering, 2008, 11, 649-660.	1.6	25
68	Estimation of volume flow in curved tubes based on analytical and computational analysis of axial velocity profiles. Physics of Fluids, 2009, 21, .	4.0	25
69	In vitro and in vivo studies on thermistorâ€based intracoronary temperature measurements: Effect of pressure and flow. Catheterization and Cardiovascular Interventions, 2009, 73, 224-230.	1.7	25
70	Accuracy and precision of vessel area assessment: Manual versus automatic lumen delineation based on fullâ€width at halfâ€maximum. Journal of Magnetic Resonance Imaging, 2012, 36, 1186-1193.	3.4	25
71	Personalization of models with many model parameters: an efficient sensitivity analysis approach. International Journal for Numerical Methods in Biomedical Engineering, 2015, 31, .	2.1	25
72	Global sensitivity analysis of a wave propagation model for arm arteries. Medical Engineering and Physics, 2011, 33, 1008-1016.	1.7	24

#	Article	IF	CITATIONS
73	Multiperspective Ultrasound Strain Imaging of the Abdominal Aorta. IEEE Transactions on Medical Imaging, 2020, 39, 3714-3724.	8.9	24
74	Medium with blood-analog mechanical properties for cardiovascular tissue culturing. Biorheology, 2008, 45, 651-661.	0.4	23
75	Clinical Study Protocol for the ARCH Project Computational Modeling for Improvement of Outcome after Vascular Access Creation. Journal of Vascular Access, 2011, 12, 369-376.	0.9	23
76	A lumped model for blood flow and pressure in the systemic arteries based on an approximate velocity profile function. Mathematical Biosciences and Engineering, 2009, 6, 27-40.	1.9	23
77	On automated analysis of flow patterns in cerebral aneurysms based on vortex identification. Journal of Engineering Mathematics, 2009, 64, 391-401.	1.2	22
78	Echo-Computed Tomography Strain Imaging of Healthy and Diseased Carotid Specimens. Ultrasound in Medicine and Biology, 2014, 40, 1329-1342.	1.5	21
79	A Constitutive Model for a Maturing Fibrin Network. Biophysical Journal, 2014, 107, 504-513.	0.5	21
80	A 1D pulse wave propagation model of the hemodynamics of calf muscle pump function. International Journal for Numerical Methods in Biomedical Engineering, 2015, 31, e02716.	2.1	21
81	Feasibility of wall stress analysis of abdominal aortic aneurysms using three-dimensional ultrasound. Journal of Vascular Surgery, 2015, 61, 1175-1184.	1.1	21
82	Automated 3D geometry segmentation of the healthy and diseased carotid artery in freeâ€hand, probe tracked ultrasound images. Medical Physics, 2020, 47, 1034-1047.	3.0	21
83	Videodensitometric quantification of paravalvular regurgitation of a transcatheter aortic valve: in vitro validation. EuroIntervention, 2018, 13, 1527-1535.	3.2	21
84	Determination of linear viscoelastic behavior of abdominal aortic aneurysm thrombus. Biorheology, 2006, 43, 695-707.	0.4	21
85	Evaluation of the haemodynamic characteristics of drug-eluting stents at implantation and at follow-up. European Heart Journal, 2006, 27, 1811-1817.	2.2	20
86	Perpendicular ultrasound velocity measurement by 2D cross correlation of RF data. Part A: validation in a straight tube. Experiments in Fluids, 2010, 49, 1177-1186.	2.4	20
87	A continuum model for platelet plug formation and growth. International Journal for Numerical Methods in Biomedical Engineering, 2014, 30, 634-658.	2.1	20
88	Enhancement of Arterial Pressure Pulsatility by Controlling Continuous-Flow Left Ventricular Assist Device Flow Rate in Mock Circulatory System. Journal of Medical and Biological Engineering, 2016, 36, 308-315.	1.8	20
89	In vitro assessment of mitral valve function in cyclically pressurized porcine hearts. Medical Engineering and Physics, 2016, 38, 346-353.	1.7	20
90	A second order splitting algorithm for thermallyâ€driven flow problems. International Journal of Numerical Methods for Heat and Fluid Flow, 1996, 6, 51-60.	2.8	19

#	Article	IF	CITATIONS
91	Improving Arterial Pulsatility by Feedback Control of a Continuous Flow Left Ventricular Assist Device via <i>in Silico</i> Modeling. International Journal of Artificial Organs, 2014, 37, 773-785.	1.4	19
92	Assessment of aortic valve pressure overload and leaflet functions in an ex vivo beating heart loaded with a continuous flow cardiac assist device. European Journal of Cardio-thoracic Surgery, 2014, 45, 377-383.	1.4	19
93	Arterial pulsatility improvement in a feedback-controlled continuous flow left ventricular assist device: An ex-vivo experimental study. Medical Engineering and Physics, 2014, 36, 1288-1295.	1.7	19
94	Diastolic Augmentation Index Improves Radial Augmentation Index in Assessing Arterial Stiffness. Scientific Reports, 2017, 7, 5864.	3.3	19
95	Towards Patient-Specific Modeling of Coronary Hemodynamics in Healthy and Diseased State. Computational and Mathematical Methods in Medicine, 2013, 2013, 1-15.	1.3	18
96	In Vitro Comparison of Support Capabilities of Intraâ€Aortic Balloon Pump and Impella 2.5 Left Percutaneous. Artificial Organs, 2011, 35, 893-901.	1.9	17
97	Modeling the Interaction Between the Intra-Aortic Balloon Pump and the Cardiovascular System. ASAIO Journal, 2013, 59, 30-36.	1.6	17
98	Assessment of mechanical properties of porcine aortas under physiological loading conditions using vascular elastography. Journal of the Mechanical Behavior of Biomedical Materials, 2016, 59, 185-196.	3.1	17
99	Vascular Elastography: A Validation Study. Ultrasound in Medicine and Biology, 2014, 40, 1882-1895.	1.5	16
100	Intraâ€Aortic Balloon Pump Support in the Isolated Beating Porcine Heart in Nonischemic and Ischemic Pump Failure. Artificial Organs, 2015, 39, 931-938.	1.9	16
101	Influence of limited field-of-view on wall stress analysis in abdominal aortic aneurysms. Journal of Biomechanics, 2016, 49, 2405-2412.	2.1	16
102	Segmentation of the left ventricle in cardiac MRI using a hierarchical extreme learning machine model. International Journal of Machine Learning and Cybernetics, 2018, 9, 1741-1751.	3.6	16
103	Computational Mesh Generation for Vascular Structures with Deformable Surfaces. International Journal of Computer Assisted Radiology and Surgery, 2006, 1, 39-49.	2.8	15
104	2H-1 In Vivo 3D Cardiac and Skeletal Muscle Strain Estimation. , 2006, , .		15
105	Assessment of endoleak significance after endovascular repair of abdominal aortic aneurysms: A lumped parameter model. Medical Engineering and Physics, 2007, 29, 1106-1118.	1.7	15
106	Perpendicular ultrasound velocity measurement by 2D cross correlation of RF data. Part B: volume flow estimation in curved vessels. Experiments in Fluids, 2010, 49, 1219-1229.	2.4	15
107	Improving the thermal dimensional stability of flexible polymer composite backing materials for ultrasound transducers. Ultrasonics, 2010, 50, 458-466.	3.9	15
108	Towards mechanical characterization of intact endarterectomy samples of carotid arteries during inflation using Echo-CT. Journal of Biomechanics, 2014, 47, 805-814.	2.1	15

#	Article	IF	CITATIONS
109	Estimation of Left Ventricular Pressure with the Pump as "Sensor―in Patients with a Continuous Flow LVAD. International Journal of Artificial Organs, 2015, 38, 433-443.	1.4	15
110	A constitutive model for the time-dependent, nonlinear stress response of fibrin networks. Biomechanics and Modeling in Mechanobiology, 2015, 14, 995-1006.	2.8	15
111	The fiber orientation in the coronary arterial wall at physiological loading evaluated with a two-fiber constitutive model. Biomechanics and Modeling in Mechanobiology, 2012, 11, 533-542.	2.8	14
112	A sensitivity analysis of a personalized pulse wave propagation model for arteriovenous fistula surgery. Part B: Identification of possible generic model parameters. Medical Engineering and Physics, 2013, 35, 827-837.	1.7	14
113	Including surrounding tissue improves ultrasound-based 3D mechanical characterization of abdominal aortic aneurysms. Journal of Biomechanics, 2019, 85, 126-133.	2.1	14
114	The influence of model order reduction on the computed fractional flow reserve using parameterized coronary geometries. Journal of Biomechanics, 2019, 82, 313-323.	2.1	14
115	Enhancing Lateral Contrast Using Multi-perspective Ultrasound Imaging of Abdominal Aortas. Ultrasound in Medicine and Biology, 2021, 47, 535-545.	1.5	14
116	A novel synchronised diastolic injection method to reduce contrast volume during aortography for aortic regurgitation assessment: in vitro experiment of a transcatheter heart valve model. EuroIntervention, 2017, 13, 1288-1295.	3.2	14
117	Ultrasound Based Wall Stress Analysis of Abdominal Aortic Aneurysms using Multiperspective Imaging. European Journal of Vascular and Endovascular Surgery, 2020, 59, 81-91.	1.5	13
118	Taylor-Galerkin-based spectral element methods for convection-diffusion problems. International Journal for Numerical Methods in Fluids, 1994, 18, 853-870.	1.6	12
119	Fast and Accurate Pressure-Drop Prediction in Straightened Atherosclerotic Coronary Arteries. Annals of Biomedical Engineering, 2015, 43, 59-67.	2.5	12
120	Intra-aortic balloon counterpulsation in acute myocardial infarction: old and emerging indications. Netherlands Heart Journal, 2013, 21, 554-560.	0.8	11
121	Autoregulation of Coronary Blood Flow in the Isolated Beating Pig Heart. Artificial Organs, 2013, 37, 724-730.	1.9	11
122	Computational modelling of endoleak after endovascular repair of abdominal aortic aneurysms. International Journal for Numerical Methods in Biomedical Engineering, 2010, 26, 322-335.	2.1	10
123	Visualization of vasculature using a hand-held photoacoustic probe: phantom and <i>in vivo</i> validation. Journal of Biomedical Optics, 2017, 22, 041013.	2.6	10
124	Intracoronary hypothermia for acute myocardial infarction in the isolated beating pig heart. American Journal of Translational Research (discontinued), 2017, 9, 558-568.	0.0	10
125	Interprofessional Consensus Regarding Design Requirements for Liquid-Based Perinatal Life Support (PLS) Technology. Frontiers in Pediatrics, 2021, 9, 793531.	1.9	10
126	A Novel Experimental Approach for Three-Dimensional Geometry Assessment of Calcified Human Stenotic Arteries inÂVitro. Ultrasound in Medicine and Biology, 2013, 39, 1875-1886.	1.5	9

#	Article	IF	CITATIONS
127	How to define the hemodynamic significance of an equivocal iliofemoral artery stenosis: Review of literature and outcomes of an international questionnaire. Vascular, 2017, 25, 598-608.	0.9	9
128	A Generalized Approach for Automatic 3-D Geometry Assessment of Blood Vessels in Transverse Ultrasound Images Using Convolutional Neural Networks. IEEE Transactions on Ultrasonics, Ferroelectrics, and Frequency Control, 2021, 68, 3326-3335.	3.0	9
129	A Novel Flexible Thermoelectric Sensor for Intravascular Flow Assessment. IEEE Sensors Journal, 2013, 13, 3883-3891.	4.7	8
130	A continuum model for platelet plug formation, growth and deformation. International Journal for Numerical Methods in Biomedical Engineering, 2014, 30, 1541-1557.	2.1	8
131	Aortic Valve Function Under Support of a Left Ventricular Assist Device: Continuous vs. Dynamic Speed Support. Annals of Biomedical Engineering, 2015, 43, 1727-1737.	2.5	8
132	An overlapping domain technique coupling spectral and finite elements for fluid–structure interaction. Computers and Fluids, 2015, 123, 235-245.	2.5	8
133	Echocardiographic Assessment of Left Bundle Branch–Related Strain Dyssynchrony: A Comparison With Tagged MRI. Ultrasound in Medicine and Biology, 2019, 45, 2063-2074.	1.5	8
134	Reproducibility assessment of ultrasound-based aortic stiffness quantification and verification using Bi-axial tensile testing. Journal of the Mechanical Behavior of Biomedical Materials, 2020, 103, 103571.	3.1	8
135	Ultrasound-Based Fluid-Structure Interaction Modeling of Abdominal Aortic Aneurysms Incorporating Pre-stress. Frontiers in Physiology, 2021, 12, 717593.	2.8	8
136	Influence of orientation of bi-leaflet valve prostheses on coronary perfusion pressure in humans. Interactive Cardiovascular and Thoracic Surgery, 2007, 6, 588-592.	1.1	7
137	On the Applicability of the Grace Curve in Practical Mixing Operations. Canadian Journal of Chemical Engineering, 2002, 80, 1-6.	1.7	7
138	Thermal anemometric assessment of coronary flow reserve with a pressure-sensing guide wire: An in vitro evaluation. Medical Engineering and Physics, 2011, 33, 684-691.	1.7	7
139	Computational model for estimating the short- and long-term cardiac response to arteriovenous fistula creation for hemodialysis. Medical and Biological Engineering and Computing, 2012, 50, 1289-1298.	2.8	7
140	Non Contrast-Enhanced MRA versus Ultrasound Blood Vessel Assessment to determine the Choice of Hemodialysis Vascular Access. Journal of Vascular Access, 2013, 14, 348-355.	0.9	7
141	Ultrasound functional imaging in an <i>ex vivo</i> beating porcine heart platform. Physics in Medicine and Biology, 2017, 62, 9112-9126.	3.0	7
142	In Vivo Validation of Patientâ€Specific Pressure Gradient Calculations for Iliac Artery Stenosis Severity Assessment. Journal of the American Heart Association, 2017, 6, .	3.7	7
143	Investigation on the Effect of Spatial Compounding on Photoacoustic Images of Carotid Plaques in the <italic>In Vivo</italic> Available Rotational Range. IEEE Transactions on Ultrasonics, Ferroelectrics, and Frequency Control, 2018, 65, 440-447.	3.0	7
144	Continuum modeling of thrombus formation and growth under different shear rates. Journal of Biomechanics, 2022, 132, 110915.	2.1	7

#	Article	IF	CITATIONS
145	Three-Dimensional Blood Flow in Bifurcations: Computational and Experimental Analyses and Clinical Applications. Cerebrovascular Diseases, 1993, 3, 185-192.	1.7	6
146	The reliability of continuous measurement of mixed venous oxygen saturation during exercise in patients with chronic heart failure. European Journal of Applied Physiology, 2008, 102, 493-496.	2.5	6
147	Computational analysis of ventricular valve–valve interaction: Influence of flow conditions. International Journal of Computational Fluid Dynamics, 2009, 23, 609-622.	1.2	6
148	An overlapping domain technique coupling spectral and finite elements for fluid flow. Computers and Fluids, 2014, 100, 336-346.	2.5	6
149	Inflation and Bi-Axial Tensile Testing of Healthy PorcineÂCarotid Arteries. Ultrasound in Medicine and Biology, 2016, 42, 574-585.	1.5	6
150	Uncertainty in modelâ€based treatment decision support: Applied to aortic valve stenosis. International Journal for Numerical Methods in Biomedical Engineering, 2020, 36, e3388.	2.1	6
151	A Spatial Near-Field Clutter Reduction Filter Preserving Tissue Speckle in Echocardiography. IEEE Transactions on Ultrasonics, Ferroelectrics, and Frequency Control, 2021, 68, 979-992.	3.0	6
152	Mechanical characterization of abdominal aortas using multi-perspective ultrasound imaging. Journal of the Mechanical Behavior of Biomedical Materials, 2021, 119, 104509.	3.1	6
153	Incompressible low-speed-ratio flow in non-uniform distensible tubes. International Journal for Numerical Methods in Fluids, 1993, 16, 597-612.	1.6	5
154	Automatic determination of the dynamic geometry of abdominal aortic aneurysm from MR with application to wall stress simulations. International Congress Series, 2005, 1281, 339-344.	0.2	5
155	The Benefit of Non Contrast-Enhanced Magnetic Resonance Angiography for Predicting Vascular Access Surgery Outcome: A Computer Model Perspective. PLoS ONE, 2013, 8, e53615.	2.5	5
156	Optical and acoustic characterization of freeze-thawed polyvinyl alcohol gels. , 2014, , .		5
157	A microscale pulsatile flow device for dynamic cross-slot rheometry. Sensors and Actuators A: Physical, 2014, 220, 221-229.	4.1	5
158	An in silico case study of idiopathic dilated cardiomyopathy via a multi-scale model of the cardiovascular system. Computers in Biology and Medicine, 2014, 53, 141-153.	7.0	5
159	Global sensitivity analysis of a model for venous valve dynamics. Journal of Biomechanics, 2016, 49, 2845-2853.	2.1	5
160	A mathematical model to simulate the cardiotocogram during labor. Part A: Model setup and simulation of late decelerations. Journal of Biomechanics, 2016, 49, 2466-2473.	2.1	5
161	A mathematical model to simulate the cardiotocogram during labor. Part B: Parameter estimation and simulation of variable decelerations. Journal of Biomechanics, 2016, 49, 2474-2480.	2.1	5
162	A predictive computational model to estimate myocardial temperature during intracoronary hypothermia in acute myocardial infarction. Medical Engineering and Physics, 2019, 68, 65-75.	1.7	5

#	Article	IF	CITATIONS
163	Image acquisition stability of fixated musculoskeletal sonography in an exercise setting: a quantitative analysis and comparison with freehand acquisition. Journal of Medical Ultrasonics (2001), 2020, 47, 47-56.	1.3	5
164	3D-printed stenotic aortic valve model to simulate physiology before, during, and after transcatheter aortic valve implantation. International Journal of Cardiology, 2020, 313, 32-34.	1.7	5
165	The Feasibility of Dynamic Musculoskeletal Function Analysis of the Vastus Lateralis in Endurance Runners Using Continuous, Hands-Free Ultrasound. Applied Sciences (Switzerland), 2021, 11, 1534.	2.5	5
166	Left Ventricular Shear Strain in Model and Experiment: The Role of Myofiber Orientation. Lecture Notes in Computer Science, 2005, , 314-324.	1.3	4
167	A computational fluid dynamics study on hemodynamics for different locations of the distal anastomosis of a bypass nearby a collateral vessel in the femoropopliteal area. International Journal for Numerical Methods in Biomedical Engineering, 2014, 30, 1263-1277.	2.1	4
168	Ex vivo photoacoustic imaging of atherosclerotic carotid plaques. , 2015, , .		4
169	Arterial pulsatility under phasic left ventricular assist device support. Bio-Medical Materials and Engineering, 2016, 27, 451-460.	0.6	4
170	Modeling regulation of vascular tone following muscle contraction: Model development, validation and global sensitivity analysis. Journal of Computational Science, 2018, 24, 143-159.	2.9	4
171	An R-Space Theorem for Plane Wave Ultrasound Reconstruction. , 2020, , .		4
172	A novel technique for the assessment of mechanical properties of vascular tissue. Biomechanics and Modeling in Mechanobiology, 2020, 19, 1585-1594.	2.8	4
173	A strategy to personalize a 1D pulse wave propagation model for estimating subject-specific central aortic pressure waveform. Computers in Biology and Medicine, 2022, 146, 105528.	7.0	4
174	Local influence of calcifications on the wall mechanics of abdominal aortic aneurysm. , 2006, , .		3
175	Plaque and Shear Stress Distribution in Human Coronary Bifurcations: a Multi-Slice Computed Tomography Study. , 2007, , 477.		3
176	A combination of thermal methods to assess coronary pressure and flow dynamics with a pressure-sensing guide wire. Medical Engineering and Physics, 2013, 35, 298-309.	1.7	3
177	Optical absorbance measurements and photoacoustic evaluation of freeze-thawed polyvinyl-alcohol vessel phantoms. Proceedings of SPIE, 2015, , .	0.8	3
178	Hemodynamic significance assessment of equivocal iliac artery stenoses by comparing duplex ultrasonography with intra-arterial pressure measurements. Journal of Cardiovascular Surgery, 2017, 59, 37-44.	0.6	3
179	Ultrasoundâ€based estimation of remaining cardiac function in LVADâ€supported ex vivo hearts. Artificial Organs, 2020, 44, E326-E336.	1.9	3
180	Personalised imaging and biomechanical modelling of large vessels. Medical and Biological Engineering and Computing, 2008, 46, 1057-1058.	2.8	2

#	Article	IF	CITATIONS
181	A longitudinal feasibility study on AAA growth vs. ultrasound elastography. , 2014, , .		2
182	Simulation of fetal heart rate variability with a mathematical model. Medical Engineering and Physics, 2017, 42, 55-64.	1.7	2
183	A mathematical model to investigate the effects of intravenous fluid administration and fluid loss. Journal of Biomechanics, 2019, 88, 4-11.	2.1	2
184	A demonstration of high field-of-view stability in hands-free echocardiography. Cardiovascular Ultrasound, 2020, 18, 18.	1.6	2
185	Multiscale modeling of a modified <scp>Blalockâ€Taussig</scp> surgery in a <scp>patientâ€specific</scp> tetralogy of Fallot. International Journal for Numerical Methods in Biomedical Engineering, 2021, 37, e3436.	2.1	2
186	Quantitative Methods for Comparisons between Velocity Encoded MR-Measurements and Finite Element Modeling in Phantom Models. Lecture Notes in Computer Science, 2002, , 255-264.	1.3	2
187	A 1D Wave Propagation Model of Coronary Flow in a Beating Heart. , 2011, , .		2
188	SVD-based filtering to detect intraplaque hemorrhage using single wavelength photoacoustic imaging. Journal of Biomedical Optics, 2021, 26, .	2.6	2
189	Patient-specific models of wall stress in abdominal aortic aneurysm: a comparison between MR and CT. , 2006, 6143, 111.		1
190	Location of Plaque Ulceration in Human Coronary Arteries is Related to Shear Stress. , 2010, , .		1
191	Correlation-based discrimination between myocardial tissue and blood in 3D echocardiographic images. , 2012, , .		1
192	Automated 2D ultrasound fusion imaging of abdominal aortic aneurysms. , 2012, , .		1
193	Response of the authors on: Comment to "Huberts W, Bode AS, Kroon W, Planken RN, Tordoir JHM, van de Vosse FN. A pulse wave propagation model to support decision-making in the clinic [Med Eng Phys 2012;34:233–48]― Medical Engineering and Physics, 2012, 34, 1029.	1.7	1
194	Design of a fatty plaque phantom for validation of strain imaging. , 2014, , .		1
195	Semi-3D strain imaging in normal and LVAD supported ex vivo beating hearts. , 2015, , .		1
196	Automatic segmentation and registration of abdominal aortic aneurysms using 3D ultrasound. , 2016, , \cdot		1
197	Notice of Removal: Characterization of human carotid plaques using multi-wavelength photoacoustic imaging. , 2017, , .		1
198	Perfusion dynamics assessment with Power Doppler ultrasound in skeletal muscle during maximal and submaximal cycling exercise. European Journal of Applied Physiology, 2018, 118, 1209-1219.	2.5	1

#	Article	IF	CITATIONS
199	Zeroâ€dimensional lumped approach to incorporate the dynamic part of the pressure at vessel junctions in a 1D wave propagation model. International Journal for Numerical Methods in Biomedical Engineering, 2018, 34, e3116.	2.1	1
200	A comparative study of geometry-based methods and intra-arterial pressure measurements to assess the hemodynamic significance of equivocal iliac artery stenoses. Vascular, 2019, 27, 119-127.	0.9	1
201	Recovery Responses of Central Hemodynamics in Basketball Athletes and Controls After the Bruce Test. Frontiers in Physiology, 2020, 11, 593277.	2.8	1
202	Model-based aortic power transfer: A potential measure for quantifying aortic stenosis severity based on measured data. Medical Engineering and Physics, 2021, 90, 66-81.	1.7	1
203	Scale-Resolving Simulations of Steady and Pulsatile Flow Through Healthy and Stenotic Heart Valves. Journal of Biomechanical Engineering, 2022, 144, .	1.3	1
204	Local Mechanical Properties of Abdominal Aortic Aneurysms. , 2008, , .		1
205	<title>LDA measurements in a nonstenosed and a stenosed model of the carotid artery bifurcation</title> . , 1993, , .		0
206	Culture Medium With Blood Analog Mechanical Properties. , 2007, , 189.		0
207	Intraluminal Thrombus in AAA Wall Stress Analysis. , 2007, , .		0
208	Mechanical Properties of the Porcine Coronary Artery. , 2008, , .		0
209	MRI Based Quantification of Outflow Boundary Conditions for Computational Fluid Dynamics of Stenosed Human Carotid Arteries. , 2010, , .		Ο
210	Response to comments on: "The Influence of WallÂStress on AAA Growth and Biomarkers― European Journal of Vascular and Endovascular Surgery, 2010, 39, 797.	1.5	0
211	Probing Red Blood Cell Dynamics. , 2012, , .		0
212	Flow Induced Vasodilation in Porcine Carotid Arteries. , 2012, , .		0
213	Wall stress analysis of abdominal aortic aneurysms using 3D ultrasound. , 2014, , .		Ο
214	A dedicated guided-search displacement algorithm for cardiovascular strain imaging. , 2014, , .		0
215	In vitro elastography of porcine carotid arteries, a validation study. , 2014, , .		Ο
216	Photoacoustic perfusion measurements: a comparison with power Doppler in phantoms. Proceedings of SPIE, 2015, , .	0.8	0

#	Article	IF	CITATIONS
217	Segmentation of the Left Ventricle in Cardiac MRI Using an ELM Model. Proceedings in Adaptation, Learning and Optimization, 2016, , 147-157.	1.6	0
218	Notice of Removal: Hemorrhages detection in atherosclerotic plaques using ultrasound and photoacoustic, phantom study. , 2017, , .		0
219	Notice of Removal: In-vivo mechanical characterization of abdominal aortic aneurysms and healthy aortas using 4D ultrasound: A comparison study. , 2017, , .		0
220	The Role of One-Dimensional Model-Generated Inter-Subject Variations in Systemic Properties on Wall Shear Stress Indices of Intracranial Aneurysms. IEEE Transactions on Biomedical Engineering, 2020, 67, 1030-1039.	4.2	0
221	Quantification of the temperature gradient through a catheter in continuous infusion thermodilution for coronary flow measurements. Physiological Measurement, 2020, 41, 075006.	2.1	0
222	In-Vitro Evaluation of Hot-Film Anemometry Using a Sensor-Tipped Coronary Guide-wire. , 2007, , .		0
223	The Mechanical Properties of Porcine Coronary Arteries Determined With a Mixed Experimental-Numerical Approach. , 2008, , .		0
224	A Time Periodic Coupling for Fluid Structure Interaction in Distensible Vessels. , 2008, , .		0
225	Feasibility of Determination of Mechanical Properties of Abdominal Aortic Aneurysms by Simultaneous Pressure and Volume Measurements In-Vivo. , 2008, , .		0
226	Growth and Remodeling of Arterial Tissue. , 2008, , .		0
227	Discrimination of Vessel Wall Components of Abdominal Aortic Aneurysms by Multi-Contrast MRI. , 2008, , .		Ο
228	Comparison of Outflow Condition Models on the Effect of Wall Shear Stress Distribution in Patient Specific Coronary Trees. , 2008, , .		0
229	99 Percentile Wall Stress and Not Peak Stress Correlates With AAA Diameter. , 2008, , .		0
230	Estimation of the Arterial Mechanical Properties Based on a Patient Specific Wave Propagation Model Using a Stochastic Method. , 2009, , .		0
231	A Mixed Experimental-Numerical Estimation Strategy to Characterize Arterial Wall Properties Including Residual Strains. , 2009, , .		Ο
232	Mechanical Properties of the Porcine Coronary Artery. , 2009, , .		0
233	Effect of Intraluminal Thrombus on Wall Stress and Growth Rate of Abdominal Aneurysms. , 2010, , .		Ο
234	Novel Strategy of the Determination of Mechanical Properties of Human Carotid Atherosclerotic Plaques. , 2012, , .		0

#	ARTICLE	IF	CITATIONS
235	Geometrical and Morphological Assessment of Human Endarterectomy Specimens In Vitro. , 2013, , .		Ο
236	Intraplaque haemorrhage detection using single-wavelength PAI and singular value decomposition in the carotid artery. , 2019, , .		0